

Effect of a finite oxide layer on the Faraday rotation and ellipticity in a metal-oxide-semiconductor system

A. Khandker, R. F. O'Connell, and G. Wallace

Department of Physics and Astronomy, Louisiana State University, Baton Rouge, Louisiana 70803

(Received 12 September 1983; revised manuscript received 24 January 1985)

We study the effect of a finite oxide layer on the Faraday rotation and ellipticity in a metal-oxide-semiconductor system. We find that the multiple internal reflections within the oxide layer can give an enhancement on the order of 21% over the case where the oxide layer is considered semi-infinite. At high magnetic fields, there is serious disagreement between theory and experiment.

Recently we calculated the Faraday rotation θ and ellipticity δ due to a two-dimensional electron gas (2DEG), in the case where the directions of both the incident radiation of frequency ω and the external dc magnetic field $B > 0$ are oriented normal to the oxide-semiconductor interface containing the 2DEG in a metal-oxide-semiconductor (MOS) system and where the oxide and semiconductor were assumed semi-infinite,¹ the latter being appropriate when a wedge is used to eliminate multiple internal reflections within the semiconductor. The effect of a finite semiconductor substrate has been shown to have a strong effect on both cyclotron resonance^{2,3} and on the Faraday rotation and ellipticity.⁴

The effect of the metal gate has also been analyzed.⁵ Because it is very thin (20–50 Å), it was pointed out that it could be treated as a two-dimensional charge layer at the interface of the vacuum and the oxide (analogous to the treatment of the inversion layer as a two-dimensional charge layer at the oxide-semiconductor interface).¹ In essence, the metal is ignored except that $(4\pi/c)$ times its two-dimensional conductivity is added to the refractive index of the oxide in considering the transmission of the radiation into the oxide. With this modification the usual Fresnel relations hold,^{4,6} as displayed, for example, in Eqs. (5a) and (5b) where we explicitly write down the Fresnel transmission and reflection coefficients for a surface containing a charge layer. While Eqs. (5a) and (5b) are general expressions, for the purposes of this paper the σ appearing therein refers to the inversion layer (and is the source of the free-carrier contribution of the inversion layer to the Faraday rotation). However, we have already shown that—in contrast to the case of the inversion layer—the two-dimensional conductivity (admittance) of the metal is negligibly small.⁵ This implies that the metallic gate essentially does not contribute any free-carrier Faraday rotation of its own. Thus, in essence, *we may ignore the metal altogether except for its contribution as a reflecting surface*, which is incorporated simply by taking into account the multiple reflections at the vacuum-oxide boundary. In other words, the reflection properties of the thin metal film do not measurably change the transmission of light from the vacuum into the oxide.

By the same token, the oxide-inversion layer boundary

can also be replaced by an oxide-silicon boundary, since the contribution of the inversion layer at the oxide-silicon interface has been taken into account separately. What we obtain is a decomposition of the “multiple-pass” rotation Θ and “multiple-pass” ellipticity Δ into the θ and δ of Ref. 1 (θ and δ include multiple reflections within the inversion layer) and a correction term due purely to multiple reflections at the oxide boundaries.

We consider the propagation of right- and left-circularly polarized light through the vacuum-SiO₂-Si system. The electric fields in the three regions are

$$\mathbf{E}_{i\pm} = E_{i\pm} e^{i(k_0 z - \omega t)} \hat{\mathbf{e}}_{\pm}, \quad \mathbf{E}_{r\pm} = E_{r\pm} e^{-i(k_0 z + \omega t)} \hat{\mathbf{e}}_{\pm} \quad (z < 0), \quad (1a)$$

$$\mathbf{E}_{u\pm} = E_{u\pm} e^{i(k_0 z - \omega t)} \hat{\mathbf{e}}_{\pm}, \quad \mathbf{E}_{v\pm} = E_{v\pm} e^{-i(k_0 z + \omega t)} \hat{\mathbf{e}}_{\pm} \quad (0 < z < d), \quad (1b)$$

$$\mathbf{E}_{t\pm} = E_{t\pm} e^{i[k_s(z-d) - \omega t]} \hat{\mathbf{e}}_{\pm} \quad (z > d) \quad (1c)$$

so that $\mathbf{E}_i = \mathbf{E}_{i+} + \mathbf{E}_{i-}$, $\mathbf{E}_r = \mathbf{E}_{r+} + \mathbf{E}_{r-}$, etc., k is the wave number in the corresponding medium and is given by

$$k_i = \frac{\omega}{c} n_i, \quad i = v, o, s \text{ or } 1, 2, 3, \quad (1d)$$

where v, o, s refers to the vacuum, oxide, or semiconductor, respectively, n_i is the index of refraction, d is the oxide thickness, and

$$\hat{\mathbf{e}}_{\pm} \equiv (\hat{\mathbf{x}} \mp i\hat{\mathbf{y}}) / \sqrt{2}. \quad (1e)$$

The boundary conditions at $z=0$ and $z=d$ are (a) continuity of the tangential component of the ac electric fields and (b) equality of the discontinuity of the ac magnetic fields and $(4\pi/c)j_{\pm} = (4\pi/c)\sigma_{\pm}E_{\pm}$, where j and σ are the surface current and conductivity of the 2DEG lo-

cated at the interface. These conditions imply, respectively, the following results (suppressing the “ \pm ” sign): for $z=0$,

$$E_i + E_r = E_u + E_v, \quad (2a)$$

$$k_v(E_i - E_r) - k_0(E_u - E_v) = 0, \quad (2b)$$

and for $z=d$,

$$E_u e^{ik_0 d} + E_v e^{-ik_0 d} = E_t, \quad (2c)$$

$$k_0(E_u e^{ik_0 d} - E_v e^{-ik_0 d}) - k_s E_t = \frac{4\pi\omega}{c^2} \sigma E_t. \quad (2d)$$

After some algebra, we find that the solution of Eq. (2) for the transmission coefficient $t_{\pm} \equiv E_{t\pm}/E_{i\pm}$ is, using Eq. (1d),

$$t_{\pm} = \frac{4n_0 n_v}{(n_v + n_0)[n_0 + n_s + (4\pi/c)\sigma_{\pm}]e^{-ik_0 d} - (n_0 - n_v)[n_0 - n_s - (4\pi/c)\sigma_{\pm}]e^{ik_0 d}}. \quad (3)$$

Equation (3) may be written as

$$t_{\pm} = \frac{t_{12} t_{23\pm} e^{ik_0 d}}{1 - r_{21} r_{23\pm} e^{2ik_0 d}}, \quad (4)$$

where^{4,6}

$$t_{ij\pm} = \frac{2n_i}{n_i + n_j + (4\pi/c)\sigma_{\pm}}, \quad (5a)$$

$$r_{ij\pm} = \frac{n_i - n_j - (4\pi/c)\sigma_{\pm}}{n_i + n_j + (4\pi/c)\sigma_{\pm}}, \quad (5b)$$

are the Fresnel transmission and reflection coefficients for a surface containing a 2DEG and $t_{ij\pm} - r_{ij\pm} = 1$. In Eqs. (4) and (5), the pair of indices (ij) denotes propagation from medium i in the direction of medium j . At the vacuum-oxide interface σ_{\pm} is zero.

It is convenient to write Eqs. (5) as

$$t_{ij\pm} \equiv |t_{ij\pm}| e^{i\xi_{ij\pm}}, \quad (6a)$$

$$r_{ij\pm} \equiv |r_{ij\pm}| e^{i\xi_{ij\pm}}. \quad (6b)$$

It has been shown^{7,8} that the multiple-pass Faraday rotation Θ and the multiple-pass ellipticity Δ are related to the transmission coefficients by

$$\frac{t_-}{t_+} = \left[\frac{1 - \Delta}{1 + \Delta} \right] e^{-2i\Theta}. \quad (7)$$

We now define η_{\pm} by

$$(1 - r_{21} r_{23\pm} e^{2ik_0 d})^{-1} \equiv |1 - r_{21} r_{23\pm} e^{2ik_0 d}|^{-1} e^{i\eta_{\pm}}. \quad (8)$$

Using Eq. (6b), we may write

$$1 - r_{21} r_{23\pm} e^{2ik_0 d} = 1 - r_{21} |r_{23\pm}| e^{i(2k_0 d + \xi_{23\pm})} \quad (9)$$

so that

$$\eta_{\pm} = \tan^{-1} \left[\frac{r_{21} |r_{23\pm}| \sin(2k_0 d + \xi_{23\pm})}{1 - r_{21} |r_{23\pm}| \cos(2k_0 d + \xi_{23\pm})} \right]. \quad (10)$$

From Eqs. (6a) and (8) we have

$$\frac{t_-}{t_+} = \left| \frac{t_-}{t_+} \right| e^{i(\xi_{23-} - \xi_{23+})} e^{i(\eta_- - \eta_+)}. \quad (11)$$

Thus, Θ may be decomposed as

$$\Theta = \theta + \theta_{MR}, \quad (12)$$

where

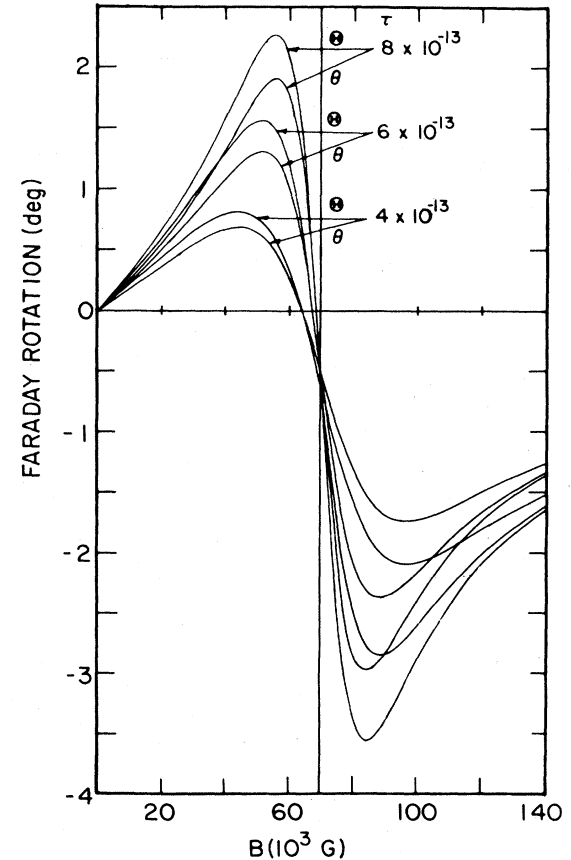


FIG. 1. Plot of the Faraday rotation Θ vs the magnetic field B . The parameters used are $N = 2.3 \times 10^{12} \text{ cm}^{-2}$, $m^* = 0.19m_e$, where m_e is the electron rest mass, $n_v = 1$, $n_0 = 1.95$, $n_s = 3.44$, $\omega = 6.455 \times 10^{12} \text{ s}^{-1}$, $d = 2000 \text{ \AA}$, and for the τ values indicated on the curves. The corresponding plots of θ are included for comparison. The vertical line corresponds to the value $\omega = \omega_c$ or $B = 6.97 \times 10^4 \text{ G}$.

$$\theta = \frac{1}{2}(\xi_{23+} - \xi_{23-}) \quad (13)$$

is the rotation studied in Ref. 1 and

$$\theta_{MR} = \frac{1}{2}(\eta_+ - \eta_-) \quad (14)$$

is the correction term for the finite thickness of the oxide layer and is due purely to multiple reflections (MR) within the oxide layer.

We emphasize that the results so far obtained are independent of the model used for the surface conductivity σ_{\pm} . We will now choose a Drude-type model, taking the surface conductivity⁶ as

$$\sigma_{\pm} = \frac{iNe^2/m^*}{\omega \pm \omega_c + i\nu}, \quad (15)$$

where N is the electron surface concentration, m^* is the effective mass, $\omega_c = eB/m^*c$ is the cyclotron frequency, and ν is the collision frequency ($=\tau^{-1}$, τ being the collision time). Thus, we obtain

$$\xi_{23\pm} = -\tan^{-1} \left[\frac{\omega_{ps}(\omega \pm \omega_c)}{(\omega \pm \omega_c)^2 + \nu(\nu + \omega_{ps})} \right], \quad (16)$$

and

$$\xi_{23\pm} = -\tan^{-1} \left[\frac{(n+1)\omega_{ps}(\omega \pm \omega_c)}{n(\omega \pm \omega_c)^2 + (n\nu - \omega_{ps})(\nu + \omega_{ps})} \right], \quad (17)$$

where

$$n \equiv \frac{n_0 - n_s}{n_0 + n_s}, \quad (18)$$

and in the notation of Ref. 6,

$$\omega_{ps} \equiv 4\pi Ne^2/m^*c(n_0 + n_s). \quad (19)$$

If $\omega_{ps} \ll$ all the other frequencies and $k_0d \ll 1$ (thin oxide layer) (which is true for parameters of physical interest), a considerable simplification occurs, viz.,

$$\xi_{23\pm} = -\frac{\omega_{ps}(\omega \pm \omega_c)}{(\omega \pm \omega_c)^2 + \nu^2}, \quad (20)$$

$$\begin{aligned} \xi_{23\pm} &= \pi - \frac{n+1}{n} \frac{\omega_{ps}(\omega \pm \omega_c)}{(\omega \pm \omega_c)^2 + \nu^2} \\ &= \pi + \frac{n+1}{n} \xi_{23\pm}, \end{aligned} \quad (21)$$

and

$$\eta_{\pm} = \frac{-r_{21} |r_{23\pm}| (2k_0d + \xi_{23\pm} - \pi)}{1 + r_{21} |r_{23\pm}|}. \quad (22)$$

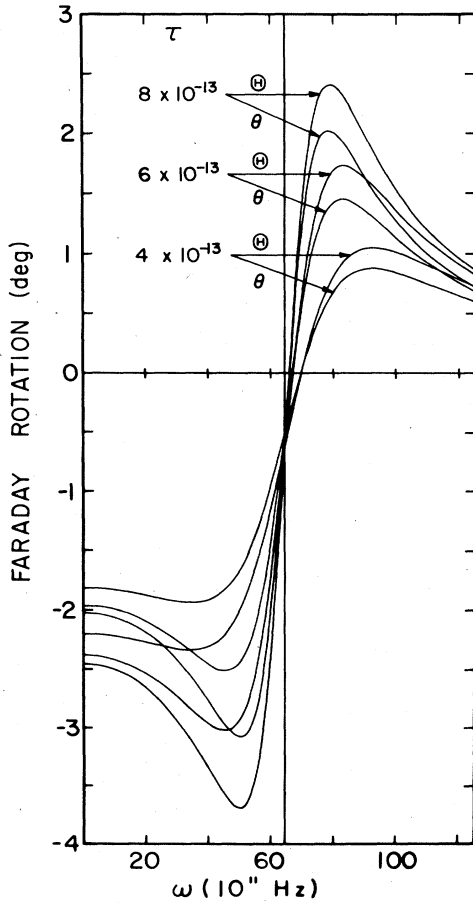


FIG. 2. Plot of the Faraday rotation Θ vs the photon frequency ω using the same parameters as in Fig. 1 and $B = 6.89 \times 10^4$ G. The vertical line corresponds to the value $\omega = \omega_c$.

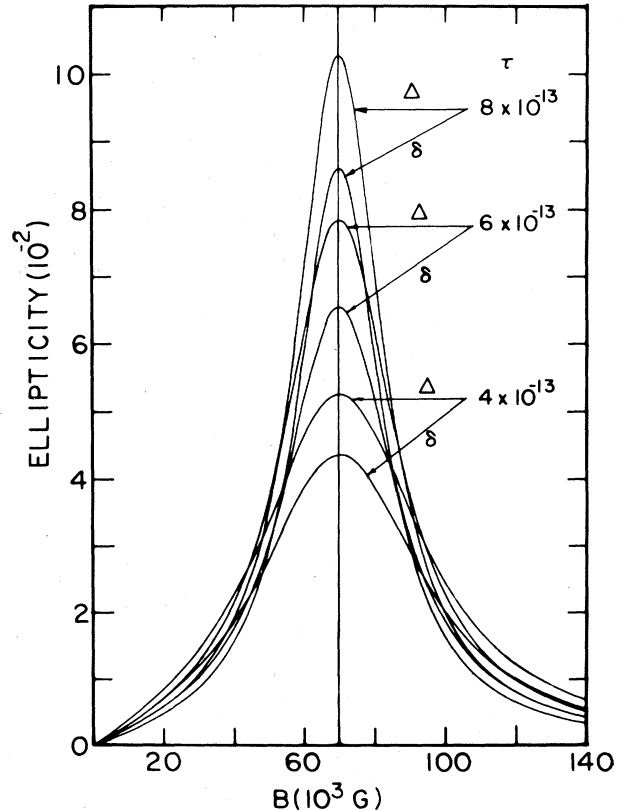


FIG. 3. Plot of the ellipticity Δ vs the magnetic field B using the same parameters as in Fig. 1.

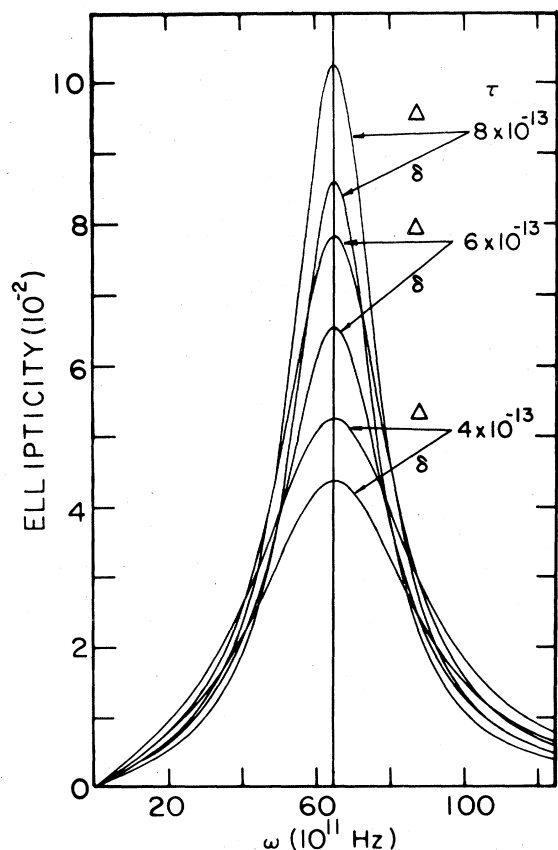


FIG. 4. Plot of the ellipticity Δ vs the photon frequency ω using the same parameters as in Fig. 2.

Thus, Eq. (14) gives

$$\theta_{MR} = \left[\frac{n_0 - n_v}{n_v + n_s} \right] \theta = \left[\frac{n_0 - 1}{1 + n_s} \right] \theta, \quad (23)$$

since $n_v = 1$ (vacuum). Hence,

$$\Theta = \theta + \theta_{MR} = \left[\frac{n_0 + n_s}{1 + n_s} \right] \theta, \quad (24)$$

where θ is given by Eqs. (13) and (20) and is the rotation studied in Ref. 1.

Using the parameters $n_0 = 1.95$ (SiO_2) and $n_s = 3.44$ (Si), Eq. (24) gives a 21% enhancement of the rotation values θ of Ref. 1, where the oxide layer was assumed to be semi-

infinite.

Using Eq. (12), we present, in Figs. 1 and 2, plots of Θ versus B and ω , respectively. The corresponding plots of θ are included for comparison.

Similar to the decomposition of Θ in Eq. (12), we obtain for the ellipticity Δ ,

$$\Delta = \frac{|t_+| - |t_-|}{|t_+| + |t_-|} = \tanh(\delta_S + \delta_{MR}), \quad (25)$$

where

$$\delta = \tanh \delta_S \quad (26)$$

is the ellipticity studied in Ref. 1 and

$$\delta_{MR} = \frac{1}{2} \ln \left| \frac{1 - r_{21} r_{23} e^{2ik_0 d}}{1 - r_{21} r_{23} e^{-2ik_0 d}} \right| \quad (27)$$

is the correction term for the finite thickness of the oxide layer and is due purely to multiple reflections. In Figs. 3 and 4, we present plots of Δ (and δ) versus B and ω , respectively, which shows the same enhancement as the rotation curves in Figs. 1 and 2.

Finally, we turn to a discussion of the comparison between our theoretical results and the experimental results recently reported by Piller and Wagner.⁹ Such a comparison was made in a recent publication¹⁰ (in a note added in proof), which for the most part was concerned with memory-function effects. In Fig. 5 of Ref. 10, we presented two "best-fit" plots of our theoretical results to the experimental results. The best agreement is obtained by the use of the Θ calculated in this paper (and corresponds to the curve labeled θ —which would have been better labeled as Θ or 1.21θ , retaining θ for the results obtained in Ref. 1). However, it is clear that *serious disagreement occurs at high magnetic fields*.

The other theoretical curve presented in Fig. 5 of Ref. 10 is labeled θ_m and corresponds to the incorporation of memory effects in the theoretical analysis. However, it will be noted that memory-function effects appear to worsen the agreement between theory and experiment.

In conclusion, it is perhaps redundant to remark on the desirability of more experimental results. In particular, a determination of the Faraday rotation for various frequencies at fixed magnetic field values would be very valuable as would ellipticity measurements.

This research was partially supported by the Department of Energy, Division of Materials Science under Grant No. DE-FG05-84ER 45135.

¹R. F. O'Connell and G. Wallace, Phys. Rev. B **26**, 2231 (1982).
²T. A. Kennedy, R. J. Wagner, B. D. McCombe, and J. J. Quinn, Solid State Commun. **18**, 275 (1976).
³G. Abstreiter, J. P. Kotthaus, J. F. Koch, and G. Dorda, Phys. Rev. B **14**, 2480 (1976).
⁴R. F. O'Connell and G. Wallace, Physica B **121**, 41 (1983).
⁵A. Khandker and R. F. O'Connell (unpublished).
⁶K. W. Chiu, T. K. Lee, and J. J. Quinn, Surf. Sci. **58**, 182 (1976).

⁷R. F. O'Connell and G. Wallace, Can. J. Phys. **61**, 49 (1983).
⁸E. D. Palik and J. K. Furdyna, Rep. Prog. Phys. **33**, 1193 (1970).
⁹H. Piller and R. J. Wagner, in *Application of High Magnetic Fields in Semiconductor Physics*, edited by G. Landwehr (Springer, Berlin, 1983), p. 199.
¹⁰R. F. O'Connell and G. Wallace, Phys. Rev. B **28**, 4643 (1983).